Accepted Manuscript

"Click" Assembly of Glycoclusters and Discovery of a Trehalose Analogue that Retards Aβ40 Aggregation and Inhibits Aβ40-Induced Neurotoxicity

Hemalatha Rajaram, Manoj Kumar Palanivelu, Thiruma V. Arumugam, Venkatesan M. Rao, P. Nicholas Shaw, Ross P. McGeary, Benjamin P. Ross

PII: S0960-894X(14)00812-9
DOI: http://dx.doi.org/10.1016/j.bmcl.2014.07.077
Reference: BMCL 21879

To appear in: *Bioorganic & Medicinal Chemistry Letters*

Received Date: 13 June 2014
Revised Date: 25 July 2014
Accepted Date: 29 July 2014

Please cite this article as: Rajaram, H., Palanivelu, M.K., Arumugam, T.V., Rao, V.M., Nicholas Shaw, P., McGeary, R.P., Ross, B.P., "Click" Assembly of Glycoclusters and Discovery of a Trehalose Analogue that Retards Aβ40 Aggregation and Inhibits Aβ40-Induced Neurotoxicity, *Bioorganic & Medicinal Chemistry Letters* (2014), doi: http://dx.doi.org/10.1016/j.bmcl.2014.07.077

"Click" Assembly of Glycoclusters and Discovery of a Trehalose Analogue that Retards Aβ40 Aggregation and Inhibits Aβ40-Induced Neurotoxicity

Hemalatha Rajaram [a], Manoj Kumar Palanivelu [a], Thiruma V. Arumugam [b], Venkatesan M. Rao [a], P. Nicholas Shaw [a], Ross P. McGeary [c], Benjamin P. Ross [a,*]

[a] The University of Queensland, School of Pharmacy, Brisbane, Queensland 4072, Australia

[b] Department of Physiology, Yong Loo Lin School Medicine, National University of Singapore, Singapore 117597, Singapore

[c] The University of Queensland, School of Chemistry and Molecular Biosciences, Brisbane, Queensland 4072, Australia

[*] Corresponding author. Tel.: +61 7 334 61900.
E-mail address: b.ross1@uq.edu.au (B.P. Ross).

Abstract:

Osmolytes have been proposed as treatments for neurodegenerative proteinopathies including Alzheimer's disease. However, for osmolytes to reach the clinic their efficacy must be improved. In this work, copper(I)-catalyzed azide-alkyne cycloaddition chemistry was used to synthesize glycoclusters bearing six copies of trehalose, lactose, galactose or glucose, with the aim of improving the potency of these osmolytes via multivalency. A trehalose glycocluster was found to be superior to monomeric trehalose in its ability to retard the formation of amyloid-beta peptide 40 (Aβ40) fibrils and protect neurons from Aβ40-induced cell death.

Keywords:

Alzheimer's disease
amyloid beta-peptides
click chemistry
glycoclusters
osmolytes

Alzheimer's disease (AD) is the most common neurodegenerative disorder and the leading cause of dementia.[1] Currently, only symptomatic treatments are available and there is an urgent need for a disease-modifying drug.[2] According to the modified amyloid cascade hypothesis,[3] AD is caused by small, soluble aggregates of amyloid-beta peptide (Aβ) which are highly neurotoxic.[4] It follows that one strategy to combat AD is to minimize the exposure of neurons to these aggregates and approaches to achieve this include: a) inhibiting the production of Aβ;[5,6] b) inhibiting Aβ aggregation;[7] c) promoting off-pathway aggregation that produces non-toxic Aβ aggregates;[8] and d) improving clearance of Aβ.[9,10]

Recently, osmolytes have been proposed as treatments for neurodegenerative proteinopathies including AD.[11] Osmolytes are small organic molecules that protect intracellular macromolecules from denaturation caused by environmental stresses such as perturbing solutes, dehydration, desiccation, extreme temperature, and high hydrostatic pressure.[12-14] There are three major categories of stabilizing osmolytes: carbohydrates; amino acids; and methylammonium/methylsulfonium compounds.[12,13] Many carbohydrate osmolytes have been found both to inhibit Aβ aggregation and to attenuate Aβ-induced neurotoxicity. Trehalose inhibits Aβ40/42 aggregation, dissociates pre-formed Aβ40/42 aggregates and decreases the toxicity of Aβ40.[15,16] Similarly, polymers carrying trehalose suppress Aβ40/42 fibril formation and reduce Aβ40/42-induced cytotoxicity.[17,18] *Myo*-, *scyllo*-, and *epi*-inositol stabilize a non-fibrillar Aβ42 structure and attenuate Aβ42-induced neurotoxicity.[19-21] Fructose inhibits fibrillogenesis of Aβ40/42[22] and attenuates Aβ42-induced neurotoxicity.[23] In many of these cases, the carbohydrate osmolytes were active at millimolar concentrations and for them to become viable treatments for AD their effectiveness must be improved. It is well established that weak interactions between proteins and carbohydrates can be amplified by constructing multivalent carbohydrate ligands and this phenomenon is known as the "cluster glycoside effect".[24,25] However, very few studies have investigated whether this phenomenon applies to carbohydrate osmolyte-Aβ interactions and then only for high MW glycopolymers.[17,18] Herein we describe the use of copper(I)-catalyzed azide-alkyne cycloaddition (CuAAC) chemistry to synthesize glycoclusters bearing six copies of trehalose, lactose, galactose or glucose, with the aim of improving the potency of the osmolytes' effect on Aβ secondary structure, aggregation, and Aβ-induced neurotoxicity.

The Scheme describes the synthesis of the glycoclusters. Dipentaerythritol (**1**) was chosen as the core branching unit onto which six mono- or disaccharides were grafted. Hexa-alkyne **2** was obtained by alkylating dipentaerythritol (**1**) with propargyl bromide under phase-transfer conditions similar to those used by Nouguier and McHich to alkylate pentraerythritol.[26] An alternative synthesis of **2** adapted from the method used by Touaibia *et al.* to alkylate pentraerythritol,[27] involving reaction of dipentaerythritol (**1**) with propargyl bromide in DMF/KOH, was inferior (6% yield) to the phase-transfer method (33% yield). Peracetylated β-glucosyl azide **3** and peracetylated β-galactosyl azide **4** were prepared from the corresponding 1,2,3,4,6-penta-*O*-acetyl-β-D-glycopyranoses by treatment with with 33% HBr in AcOH to form the 2,3,4,6-tetra-*O*-acetyl-α-D-glycopyranosyl bromides, followed by immediate nucleophilic displacement with NaN_3 in a phase-transfer reaction according to the method of Tropper *et al.*[28] Peracetylated β-lactosyl azide **5** was synthesized by first acetylating lactose with Ac_2O/NaOAc and recrystallizing the crude product from hot MeOH to give 1,2,3,6-tetra-*O*-acetyl-4-*O*-(2,3,4,6-tetra-*O*-acetyl-β-D-

galactopyranosyl)-β-D-glucopyranose.[29] This compound was converted to 2,3,6-tri-*O*-acetyl-4-*O*-(2,3,4,6-tetra-*O*-acetyl-β-D-galactopyranosyl)-α-D-glucopyranosyl bromide by treatment with 33% HBr in AcOH, followed by immediate reaction with NaN_3 in DMF to afford azide **5**.[30] Peracetylated 6-azido-6-deoxy trehalose **6** was prepared from trehalose which was iodinated with Ph_3P/I_2 followed by immediate acetylation with Ac_2O/pyridine to form 1-*O*-(2,3,4,6-tetra-*O*-acetyl-α-D-glucopyranosyl)-2,3,4-tri-*O*-acetyl-6-deoxy-6-iodo-α-D-glucopyranoside.[18] This compound was then reacted with NaN_3 in DMF to obtain azide **6**.[18] Azides **3**-**6** were "clicked" onto hexa-alkyne **2** by a CuAAC reaction[31,32] followed by Zemplén deacetylation[33] to afford the target glycoclusters **7**–**10**.

The effect of glycoclusters **7**–**10** on Aβ40 aggregation kinetics, secondary structure, fibril morphology and neurotoxicity was evaluated using the thioflavin T (ThT) fluorescence assay, circular dichroism (CD) spectroscopy, transmission electron microscopy (TEM), and the cell-based trypan blue dye exclusion assay. Control glucose, galactose, lactose, and trehalose were tested at concentrations six times greater than the glycoclusters (**7**–**10**) to ensure an equivalent concentration of mono- and disaccharide units. To obtain accurate and precise data from biophysical and biochemical experiments using Aβ, it is important to remove aggregates and prepare monomer-rich starting solutions of Aβ, commonly referred to as low molecular weight (LMW) Aβ.[34,35] However, the high tendency of Aβ to aggregate makes this a challenging task.[35] In this study, LMW Aβ40 was prepared by a facile procedure involving dissolution of Aβ40 in dilute aqueous NaOH solution (pH 10.5–12)[35] followed by dilution in phosphate buffer (pH 7.4), sonication for 60 s, and ultracentrifugation (80000 rpm for 90 min at 4ºC). As described below, the supernatant obtained from this procedure exhibited properties consistent with LMW Aβ including a sigmoidal kinetic growth curve with a long lag phase.

Glycoclusters **7**–**10** were screened for their effect on Aβ40 aggregation using a continuous ThT assay under quiescent conditions at pH 7.4 and 37 °C. ThT undergoes a large enhancement of its fluorescence emission upon binding to amyloid fibrils hence ThT fluorescence can be used to monitor Aβ aggregation.[36,37] A concentration range of 10 nM to 100 μM of glycocluster was chosen for screening because these concentrations might enable identification of potent compounds that are amenable to drug development. Aβ40 (35 μM) exhibited a sigmoidal kinetic growth curve (Figure 1) consistent with an autocatalytic process in which new oligomers initially form only via slow primary nucleation, and after elongation produces fibrils, fast fibril-catalyzed secondary nucleation commences and combines with elongation to generate new fibrils.[38,39] This autocatalytic positive feedback loop results in exponential growth and secondary nucleation dominating primary nucleation as the main source of new oligomers.[38,39] An empirical sigmoidal model was fitted to each of the fluorescence intensity versus time data sets and the amplitude and lag time were estimated.[40] Figure 2 shows the average results of four independent experiments. All of the compounds extended the lag phase of Aβ40 aggregation with a concentration-dependent increase in lag time observed for most compounds. In general, glycoclusters (**7**–**10**) at the two highest concentrations (10 μM and 100 μM) extended the lag phase more than the corresponding mono- and disaccharides (60 μM and 600 μM), and all of the glycoclusters (**7**–**10**) exhibited statistically significant activity at 100 μM with lag times increased by between 28% and 53%. Three instances of statistically significant changes in the amplitude of Aβ40 aggregation were observed,

however the differences were only small (~10%). Generally, the compounds did not effect the amplitude (Figure 1 and Figure 2), indicating that ultimately the same amount of fibrils is present at equilibrium.[41]

The extension of the lag phase of Aβ40 aggregation caused by trehalose glycocluster **10** was clearly concentration-dependent, and 100 μM of **10** resulted in an extremely significant ($p < 0.0001$) 45% increase in lag time (Figure 1 and Figure 2), consequently trehalose glycocluster **10** was chosen for further investigation. Figure 1 demonstrates that the lag phase of Aβ40 aggregation is extended as the concentration of **10** increases from 1 to 100 μM; the slope of the curve, however, remains constant. Hence, once the concentration of fibrils reaches a threshold level, the rate of fibril formation is the same and independent of the lag time.[42] Although the lag time and slope are each determined by both nucleation and growth processes,[41] the combination of an increase in lag time with no change in slope suggests that trehalose glycocluster **10** inhibits the rate of primary nucleation, with no or only a minor effect on secondary nucleation and elongation.[42]

CD spectroscopy was used to confirm the results of the ThT assay and to determine the secondary structure of the aggregates. This technique relies on the well-established principle that LMW Aβ with predominantly unordered structure[43] transitions to β-sheet rich aggregates,[34,44] and it has previously been used to study inhibition of Aβ aggregation.[45] Trehalose glycocluster **10** was incubated with Aβ40 at molar ratios of 1:5, 1:1 and 5:1 under quiescent conditions at pH 7.4 and 37 °C. The CD spectra were recorded over the wavelength range 190–250 nm and deconvoluted using the CONTIN algorithm[46,47] on the DICHROWEB server.[48] Table 1 shows the percentage of each secondary structural motif at 0 and 72 h for each sample. Initially, Aβ40 had primarily (82–87%) unordered secondary structure with negligible (0–3%) β-structure (β-sheet and β-turn) and a small (11–15%) α-helical component. These results are consistent with previous studies, which showed that LMW Aβ lacks significant ordered structure, and that transient α-helix-containing intermediates occur "on-pathway" to the formation of β-structure rich fibrils.[34,44] After 72 h, the Aβ40 control sample transitioned to predominantly (70%) β-structure with only small unordered (12%) and α-helical (18%) components, consistent with prior studies.[34,44] Trehalose had little effect on the β-structure content (65–69%), and trehalose glycocluster **10** at the two lowest concentrations was only marginally more active (62% β-structure). However, the sample containing trehalose glycocluster **10** at a ratio of 5:1 (**10**:Aβ40) displayed substantially less β-structure content (42%) and more unordered (36%) and α-helical (22%) secondary structure compared to Aβ40 control. This confirms the results of the ThT assay, that trehalose glycocluster **10** delays but does not prevent the eventual formation of Aβ40 fibrils that are rich in β-structure.

The morphology of the Aβ40 fibrils at equilibrium was studied using TEM. Trehalose glycocluster **10** was incubated with Aβ40 at molar ratios of 1:5, 1:1 and 5:1 under quiescent conditions at pH 7.4 and 37 °C for 7 days. Fibrils averaging ~12 nm in width and > 2 μm long were observed for Aβ40 alone and when Aβ40 was incubated with trehalose (Figure 3). Trehalose glycocluster **10** had a subtle effect on the fibril morphology, with slightly smaller average fibril width (~9 nm) and a significant number of shorter (< 2 μm) fibrils observed, and this effect was most pronounced in the sample containing the highest concentration of **10** (Figure 3). Taken together, the results of the ThT, CD and TEM studies reveal that the principal effect of trehalose

glycocluster **10** is inhibition of the rate of primary nucleation, with no significant effect on the thermodynamic equilibrium of Aβ40 aggregation.

The preferential exclusion of osmolyte (preferential hydration of protein) theory explains the mechanism by which osmolytes protect folded proteins from denaturation.[49,50] It states that osmolytes raise the Gibbs energy of the unfolded denatured state more than they do the folded state,[49,50] because of unfavorable interactions between the osmolyte and the peptide backbone, which is much more exposed in the unfolded state than in the folded state.[51] This solvophobic thermodynamic force, called the osmophobic effect, means that protein denaturation in the presence of osmolyte is more unfavorable than it is in the absence of osmolyte and hence osmolytes promote the folded form of the protein.[52] High-resolution NMR spectroscopy showed that in aqueous solution, synthetic Aβ40 adopts a compact, partially folded structure in which residues 13–23 form a helix and the N- and C-termini, which contain many bends and turns, are collapsed against the central helix.[53] CD spectroscopy indicates that synthetic Aβ initially has predominantly unordered secondary structure, and the α-helical content increases with time reaching maximal levels of 19–32% before waning as aggregation proceeds.[34,44] It is well established that eventually, Aβ transitions into aggregates that are rich in β-structure.[34,44,54-57] In this study, trehalose glycocluster **10** incubated with Aβ40 at a ratio of 5:1 (**10**:Aβ40) for 72 h displayed substantially less β-structure content (42%) and more unordered (36%) and α-helical (22%) secondary structure compared to Aβ40 control (Table 1). Hence, preferential exclusion of trehalose glycocluster **10** due to the osmophobic effect may stabilize a compact helical form of Aβ40 and retard the unfavorable exposure of the peptide backbone that is required for the conformational transition to β-structure.[58] This may also inhibit the rate of primary nucleation, resulting in an extended lag phase (Figure 1 and Figure 2). These explanations are consistent with molecular dynamics simulations which showed that preferential exclusion of trehalose is the origin of its inhibition of Aβ40 aggregation, partly due to stabilization of monomers with α-helical structure so that β-sheet structure is prevented.[59] Compounds that retard Aβ aggregation by stabilizing helical structure may be of therapeutic benefit in AD because nascent Aβ generated by γ-secretase cleavage of transmembrane protein C99 ($APP_{672-770}$, also called β-CTF) is likely to comprise substantial helical content, since residues 17–23 of Aβ arise from the C99 "N-helix" ($APP_{688-694}$) and residues 29–40/42 of Aβ ($APP_{700-711/713}$) originate from within the C99 helical transmembrane domain ($APP_{700-723}$).[60]

The effect of trehalose glycocluster **10** on Aβ40-induced neurotoxicity was studied using a cell-based trypan blue dye exclusion assay.[61] Preliminary studies confirmed that the test compounds alone were devoid of any inherent toxicity at the concentrations used in this study. Trehalose glycocluster **10** was incubated with Aβ40 for 6 h at 37 °C at molar ratios of 1:1 and 2.5:1 (**10**:Aβ40) prior to addition to 7–9 day old cultured mouse primary cortical neurons. After 48 h the cells were fixed with trypan blue dye and the number of alive and dead cells were counted (Figure 4). The normal control cell death was very low at 10% and oligomeric Aβ40-induced cell death was 56%. Both trehalose glycocluster **10** and trehalose[15] were neuroprotective with the greatest and most significant activity observed with 100 μM of trehalose glycocluster **10**. The percentage of neuroprotection observed with trehalose glycocluster **10** at 40 μM and 100μM was 45% and 59% respectively, and with trehalose at 240 μM and 600 μM the neuroprotection was 39% and 55% respectively.

The mechanism of neuroprotection may be attributed to the ability of trehalose glycocluster **10** to inhibit primary nucleation resulting in the formation of fewer toxic Aβ aggregates during the 6 h incubation period used in the study. However, trehalose was also neuroprotective despite trehalose not exhibiting significant activity in the ThT fluorescence assay and the CD spectroscopy study. Trehalose is an activator of autophagy[62] and increased autophagy has been found to reduce Aβ levels and improve cognitive function in a mouse model of AD,[63] therefore further work is required to elucidate the precise mechanism of the neuroprotection observed in this study. Retardation of Aβ fibril formation in combination with enhanced clearance of Aβ due to activation of autophagy may be beneficial in the treatment of AD.[62]

In conclusion, we utilized CuAAC chemistry to synthesize glycoclusters bearing six copies of carbohydrate osmolytes and discovered that a trehalose glycocluster (**10**) is superior to monomeric trehalose in its ability to retard the formation of Aβ40 fibrils and protect neurons from Aβ40-induced cell death. This work may stimulate interest in the development of osmolyte analogues including multivalent molecules as potential treatments for neurodegenerative proteinopathies.

Acknowledgements

This work was supported by grants from the Clive and Vera Ramaciotti Foundations, the Brain Foundation – Rex Banks Estate, and The University of Queensland (UQ). H.R., M.K.P., and V.M.R. thank UQ for PhD scholarships. M.K.P. thanks the Australian Government for an Endeavour Scholarship. H.R. thanks the Solander Program for a travel grant. B.P.R., H.R. and M.K.P. thank: Prof. Sara Linse and Birgitta Frohm, Lund University, for helpful discussions; Dr Tri Le, UQ, for assistance with NMR spectroscopy; Dr Ian Lane, UQ, for assistance with CD spectroscopy; and Rick Webb, UQ, for assistance with TEM. The authors acknowledge the facilities, and the scientific and technical assistance, of the Australian Microscopy & Microanalysis Research Facility at the Centre for Microscopy and Microanalysis, UQ.

Supplementary data

Supplementary data associated with this article (including novel and literature-derived[18,26-30,35,40,46,48,61,64-66] experimental content) can be found, in the online version, at

References

1. Prince, M.; Jackson, J. *Alzheimer's Disease International World Alzheimer Report 2009* **2009**.
2. Biran, Y.; Masters, C. L.; Barnham, K. J.; Bush, A. I.; Adlard, P. A. *J. Cell. Mol. Med.* **2009,** *13*, 61.
3. Hardy, J.; Selkoe, D. J. *Science* **2002,** *297*, 353.
4. Dahlgren, K. N.; Manelli, A. M.; Stine, W. B., Jr.; Baker, L. K.; Krafft, G. A.; LaDu, M. J. *J. Biol. Chem.* **2002,** *277*, 32046.
5. Chang, K.-A.; Kim, S.-H.; Kim, H.-S.; Park, C.-W.; Suh, Y.-H. *J. Mol. Neurosci.* **1999,** *12*, 69.

6. Dovey, H. F.; John, V.; Anderson, J. P.; Chen, L. Z.; de Saint Andrieu, P.; Fang, L. Y.; Freedman, S. B.; Folmer, B.; Goldbach, E.; Holsztynska, E. J.; Hu, K. L.; Johnson-Wood, K. L.; Kennedy, S. L.; Kholodenko, D.; Knops, J. E.; Latimer, L. H.; Lee, M.; Liao, Z.; Lieberburg, I. M.; Motter, R. N.; Mutter, L. C.; Nietz, J.; Quinn, K. P.; Sacchi, K. L.; Seubert, P. A.; Shopp, G. M.; Thorsett, E. D.; Tung, J. S.; Wu, J.; Yang, S.; Yin, C. T.; Schenk, D. B.; May, P. C.; Altstiel, L. D.; Bender, M. H.; Boggs, L. N.; Britton, T. C.; Clemens, J. C.; Czilli, D. L.; Dieckman-McGinty, D. K.; Droste, J. J.; Fuson, K. S.; Gitter, B. D.; Hyslop, P. A.; Johnstone, E. M.; Li, W. Y.; Little, S. P.; Mabry, T. E.; Miller, F. D.; Audia, J. E. *J. Neurochem.* **2001,** *76*, 173.
7. Tomiyama, T.; Asano, S.; Suwa, Y.; Morita, T.; Kataoka, K.; Mori, H.; Endo, N. *Biochem. Biophys. Res. Commun.* **1994,** *204*, 76.
8. Ehrnhoefer, D. E.; Bieschke, J.; Boeddrich, A.; Herbst, M.; Masino, L.; Lurz, R.; Engemann, S.; Pastore, A.; Wanker, E. E. *Nat. Struct. Mol. Biol.* **2008,** *15*, 558.
9. Schenk, D.; Barbour, R.; Dunn, W.; Gordon, G.; Grajeda, H.; Guido, T.; Hu, K.; Huang, J.; Johnson-Wood, K.; Khan, K.; Kholodenko, D.; Lee, M.; Liao, Z.; Lieberburg, I.; Motter, R.; Mutter, L.; Soriano, F.; Shopp, G.; Vasquez, N.; Vandevert, C.; Walker, S.; Wogulis, M.; Yednock, T.; Games, D.; Seubert, P. *Nature* **1999,** *400*, 173.
10. Leissring, M. A.; Farris, W.; Chang, A. Y.; Walsh, D. M.; Wu, X.; Sun, X.; Frosch, M. P.; Selkoe, D. J. *Neuron* **2003,** *40*, 1087.
11. Gross, D. S.; Klein, R. L.; Witt, S. N. In *Protein Chaperones and Protection from Neurodegenerative Diseases*; John Wiley & Sons, Inc., 2011; pp. 385-421.
12. Yancey, P. H.; Clark, M. E.; Hand, S. C.; Bowlus, R. D.; Somero, G. N. *Science* **1982,** *217*, 1214.
13. Yancey, P. H. *J. Exp. Biol.* **2005,** *208*, 2819.
14. Bolen, D. W. In *Protein Structure, Stability, and Folding;* Murphy, K. Ed.; Humana Press, 2001; pp. 17-36.
15. Liu, R.; Barkhordarian, H.; Emadi, S.; Park, C. B.; Sierks, M. R. *Neurobiol. Dis.* **2005,** *20*, 74.
16. Qi, W.; Zhang, A.; Good, T. A.; Fernandez, E. J. *Biochemistry* **2009,** *48*, 8908.
17. Miura, Y.; You, C.; Ohnishi, R. *Sci. Technol. Adv. Mater.* **2008,** *9*, 024407.
18. Wada, M.; Miyazawa, Y.; Miura, Y. *Polym. Chem.* **2011,** *2*, 1822.
19. McLaurin, J.; Golomb, R.; Jurewicz, A.; Antel, J. P.; Fraser, P. E. *J. Biol. Chem.* **2000,** *275*, 18495.
20. McLaurin, J.; Franklin, T.; Chakrabartty, A.; Fraser, P. E. *J. Mol. Biol.* **1998,** *278*, 183.
21. Townsend, M.; Cleary, J. P.; Mehta, T.; Hofmeister, J.; Lesne, S.; O'Hare, E.; Walsh, D. M.; Selkoe, D. J. *Ann. Neurol.* **2006,** *60*, 668.
22. Fung, J.; Darabie, A. A.; McLaurin, J. *Biochem. Biophys. Res. Commun.* **2005,** *328*, 1067.
23. Fernandez-Busquets, X.; Ponce, J.; Bravo, R.; Arimon, M.; Martianez, T.; Gella, A.; Cladera, J.; Durany, N. *Curr. Alzheimer Res.* **2010,** *7*, 428.
24. Lundquist, J. J.; Toone, E. J. *Chem. Rev. (Washington, DC, U. S.)* **2002,** *102*, 555.
25. Lee, Y. C.; Lee, R. T. *Acc. Chem. Res.* **1995,** *28*, 321.
26. Nouguier, R. M.; McHich, M. *J. Org. Chem.* **1985,** *50*, 3296.

27. Touaibia, M.; Wellens, A.; Shiao, T. C.; Wang, Q.; Sirois, S.; Bouckaert, J.; Roy, R. *ChemMedChem* **2007,** *2*, 1190.
28. Tropper, F. D.; Andersson, F. O.; Braun, S.; Roy, R. *Synthesis* **1992,** *1992*, 618.
29. Hudson, C. S.; Johnson, J. M. *J. Am. Chem. Soc.* **1915,** *37*, 1270.
30. Dunstan, D.; Hough, L. *Carbohydr. Res.* **1972,** *23*, 17.
31. Tornøe, C. W.; Christensen, C.; Meldal, M. *J. Org. Chem.* **2002,** *67*, 3057.
32. Rostovtsev, V. V.; Green, L. G.; Fokin, V. V.; Sharpless, K. B. *Angew. Chem. Int. Ed.* **2002,** *41*, 2596.
33. Zemplén, G. *Ber. dtsch. Chem. Ges. A/B* **1926,** *59*, 1254.
34. Walsh, D. M.; Hartley, D. M.; Kusumoto, Y.; Fezoui, Y.; Condron, M. M.; Lomakin, A.; Benedek, G. B.; Selkoe, D. J.; Teplow, D. B. *J. Biol. Chem.* **1999,** *274*, 25945.
35. Teplow, D. B. *Methods Enzymol.* **2006,** *413*, 20.
36. LeVine, H., 3rd. *Protein Sci.* **1993,** *2*, 404.
37. Biancalana, M.; Koide, S. *Biochim. Biophys. Acta* **2010,** *1804*, 1405.
38. Cohen, S. I.; Linse, S.; Luheshi, L. M.; Hellstrand, E.; White, D. A.; Rajah, L.; Otzen, D. E.; Vendruscolo, M.; Dobson, C. M.; Knowles, T. P. *Proc. Natl. Acad. Sci. U. S. A.* **2013,** *110*, 9758.
39. Arosio, P.; Cukalevski, R.; Frohm, B.; Knowles, T. P.; Linse, S. *J. Am. Chem. Soc.* **2014,** *136*, 219.
40. Hellstrand, E.; Boland, B.; Walsh, D. M.; Linse, S. *ACS Chem. Neurosci.* **2010,** *1*, 13.
41. Cohen, S. I.; Vendruscolo, M.; Dobson, C. M.; Knowles, T. P. *J. Mol. Biol.* **2012,** *421*, 160.
42. Assarsson, A.; Hellstrand, E.; Cabaleiro-Lago, C.; Linse, S. *ACS Chem. Neurosci.* **2014,** *5*, 266.
43. Sreerama, N.; Woody, R. W. *J. Mol. Biol.* **1994,** *242*, 497.
44. Kirkitadze, M. D.; Condron, M. M.; Teplow, D. B. *J. Mol. Biol.* **2001,** *312*, 1103.
45. Bartolini, M.; Bertucci, C.; Bolognesi, M. L.; Cavalli, A.; Melchiorre, C.; Andrisano, V. *ChemBioChem* **2007,** *8*, 2152.
46. Provencher, S. W.; Gloeckner, J. *Biochemistry* **1981,** *20*, 33.
47. van Stokkum, I. H. M.; Spoelder, H. J. W.; Bloemendal, M.; van Grondelle, R.; Groen, F. C. A. *Anal. Biochem.* **1990,** *191*, 110.
48. Whitmore, L.; Wallace, B. A. *Biopolymers* **2008,** *89*, 392.
49. Gekko, K.; Timasheff, S. N. *Biochemistry* **1981,** *20*, 4667.
50. Lee, J. C.; Timasheff, S. N. *J. Biol. Chem.* **1981,** *256*, 7193.
51. Liu, Y.; Bolen, D. W. *Biochemistry* **1995,** *34*, 12884.
52. Bolen, D. W.; Baskakov, I. V. *J. Mol. Biol.* **2001,** *310*, 955.
53. Vivekanandan, S.; Brender, J. R.; Lee, S. Y.; Ramamoorthy, A. *Biochem. Biophys. Res. Commun.* **2011,** *411*, 312.
54. Luhrs, T.; Ritter, C.; Adrian, M.; Riek-Loher, D.; Bohrmann, B.; Dobeli, H.; Schubert, D.; Riek, R. *Proc. Natl. Acad. Sci. U. S. A.* **2005,** *102*, 17342.
55. Paravastu, A. K.; Leapman, R. D.; Yau, W. M.; Tycko, R. *Proc. Natl. Acad. Sci. U. S. A.* **2008,** *105*, 18349.
56. Choo, L. P.; Wetzel, D. L.; Halliday, W. C.; Jackson, M.; LeVine, S. M.; Mantsch, H. H. *Biophys. J.* **1996,** *71*, 1672.
57. Lu, J. X.; Qiang, W.; Yau, W. M.; Schwieters, C. D.; Meredith, S. C.; Tycko, R. *Cell* **2013,** *154*, 1257.

58. Eisenberg, D.; Jucker, M. *Cell* **2012,** *148*, 1188.
59. Liu, F. F.; Ji, L.; Dong, X. Y.; Sun, Y. *J. Phys. Chem. B* **2009,** *113*, 11320.
60. Barrett, P. J.; Song, Y.; Van Horn, W. D.; Hustedt, E. J.; Schafer, J. M.; Hadziselimovic, A.; Beel, A. J.; Sanders, C. R. *Science* **2012,** *336*, 1168.
61. Thundyil, J.; Tang, S. C.; Okun, E.; Shah, K.; Karamyan, V. T.; Li, Y. I.; Woodruff, T. M.; Taylor, S. M.; Jo, D. G.; Mattson, M. P.; Arumugam, T. V. *Exp. Transl. Stroke Med.* **2010,** *2*, 15.
62. Sarkar, S.; Davies, J. E.; Huang, Z.; Tunnacliffe, A.; Rubinsztein, D. C. *J. Biol. Chem.* **2007,** *282*, 5641.
63. Spilman, P.; Podlutskaya, N.; Hart, M. J.; Debnath, J.; Gorostiza, O.; Bredesen, D.; Richardson, A.; Strong, R.; Galvan, V. *PLoS One* **2010,** *5*, e9979.
64. Gottlieb, H. E.; Kotlyar, V.; Nudelman, A. *J. Org. Chem.* **1997,** *62*, 7512.
65. Hronowski, L. J. J.; Szarek, W. A.; Hay, G. W.; Krebs, A.; Depew, W. T. *Carbohydr. Res.* **1989,** *190*, 203.
66. Pace, C. N.; Vajdos, F.; Fee, L.; Grimsley, G.; Gray, T. *Protein Sci.* **1995,** *4*, 2411.

Scheme. Synthesis of the glycoclusters. a) Propargyl bromide, NaOH, TBAB, toluene/water, 80°C, 16 h, 33% yield; b) i) Azides **3**–**6**, $CuSO_4$, sodium ascorbate, THF/water, 40°C, 6–18 h, ii) 10 mM NaOMe in MeOH, 3 h, iii) Amberlite IR-120(H^+), yields 56%* (**7**), 63%* (**8**), 28%** (**9**), 20%** (**10**), *purification by silica flash column chromatography, **purification by RP-HPLC.

Figure 1. Aggregation of Aβ40 monitored by *in situ* ThT fluorescence. Aβ40 (35 μM) was incubated with or without trehalose glycocluster **10** in phosphate buffer (20 mM, pH 7.4, *I* 0.15 M, containing 20 μM ThT and 0.007% NaN_3) at 37 °C under quiescent conditions. Fluorescence readings (λ_{ex} 440 nm, λ_{em} 480 nm) were taken every 5 mins. Four representative kinetic traces are shown for each group.

Figure 2. ThT assay lag times and amplitudes obtained by fitting an empirical sigmoidal model to the fluorescence intensity versus time data using non-linear regression. The dashed horizontal lines show the control Aβ40 (35 μM) value. Values are the mean + SE of four independent experiments with *p < 0.05, **p < 0.01, ***p < 0.001 and ****p < 0.0001 c.f. control. Trehalose was tested at concentrations six times greater than trehalose glycocluster **10** to ensure an equivalent concentration of trehalose units.

Figure 3. Morphology of Aβ40 fibrils after 7 days of incubation. TEM images of: a) Control Aβ40 (60 μM), fibril width 12.3 ± 1.2 nm; b) Aβ40 (60 μM) + trehalose (1800 μM), fibril width 11.8 ± 1.2 nm; and c) Aβ40 (60 μM) + trehalose glycocluster **10** (300 μM), fibril width 8.7 ± 1.1 nm. Values are the mean ± SD and the scale bar represents 200 nm. In all of the samples the majority of the fibrils were > 2 μm long however the sample containing trehalose glycocluster **10** (300 μM) exhibited a significant number of shorter (< 2 μm) fibrils. Trehalose was tested at concentrations six times greater than trehalose glycocluster **10** to ensure an equivalent concentration of trehalose units.

Figure 4. The effect of trehalose glycocluster **10** and trehalose on Aβ40-induced death of cultured mouse primary cortical neurons. Cultures were obtained from 6 biologically different pregnant C57BL/6 mice bearing 6–9 pups each. Aβ40 (40 μM) was incubated with or without test compound for 6 h at 37 °C then added to the neurons and after 48 h cell death was determined by the trypan blue exclusion assay. The values are mean + SE with *p < 0.05, **p < 0.01, and ***p < 0.001 c.f. Aβ40. Trehalose was tested at concentrations six times greater than trehalose glycocluster **10** to ensure an equivalent concentration of trehalose units.

Table 1
Conformation of Aβ40 determined by deconvolution of CD spectra using the CONTIN algorithm.

Sample	Concn [μM]	Time [h]	α-helix [%]	β-sheet [%]	β-turn [%]	Unordered [%]
Aβ40	30	0	13	2	0	85
		72	18	40	30	12
Aβ40 (30 μM)	6	0	15	1	0	84
+ glycocluster		72	21	35	27	17
10	30	0	13	0	0	87
		72	20	32	30	18
	150	0	11	2	0	87
		72	22	16	26	36
Aβ40 (30 μM)	36	0	15	3	0	82
+ trehalose[a]		72	19	36	30	15
	180	0	14	3	0	83
		72	26	36	33	5
	900	0	13	2	0	85
		72	18	36	29	17

[a] Trehalose was tested at concentrations six times greater than trehalose glycocluster **10** to ensure an equivalent concentration of trehalose units.

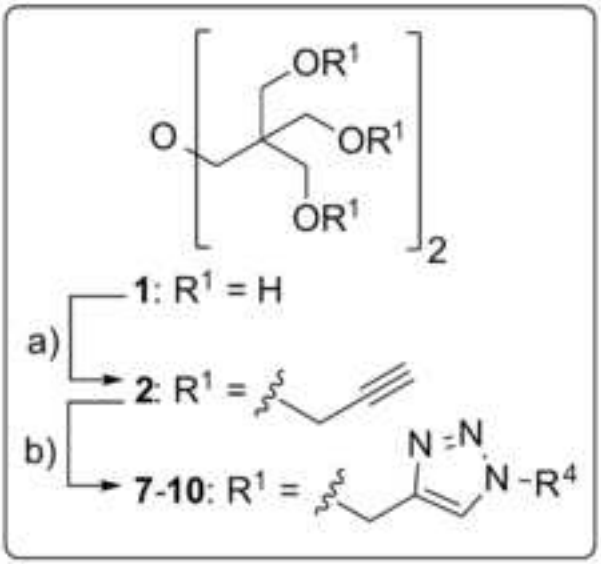

Glucose and galactose derivatives

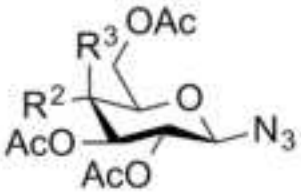

3: R^2 = OAc, R^3 = H
4: R^2 = H, R^3 = OAc

7, **8**: R^4 =

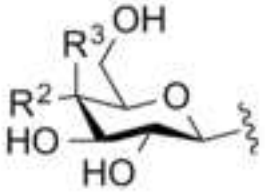

7: R^2 = OH, R^3 = H
8: R^2 = H, R^3 = OAc

Lactose derivatives

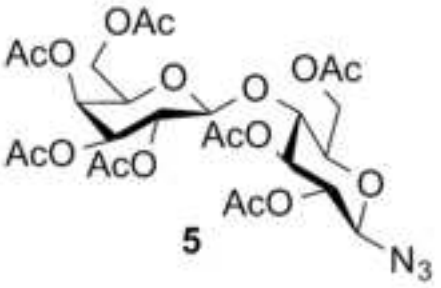

5

9: R^4 =

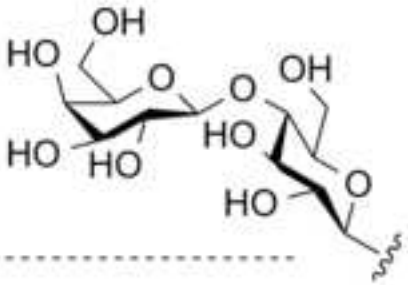

Trehalose derivatives

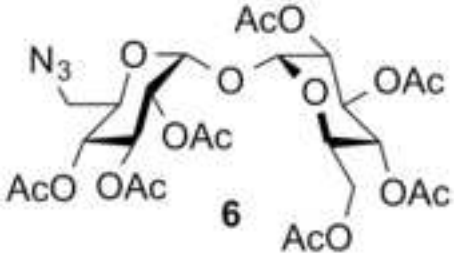

6

10: R^4 =

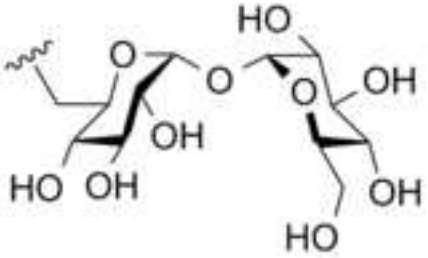

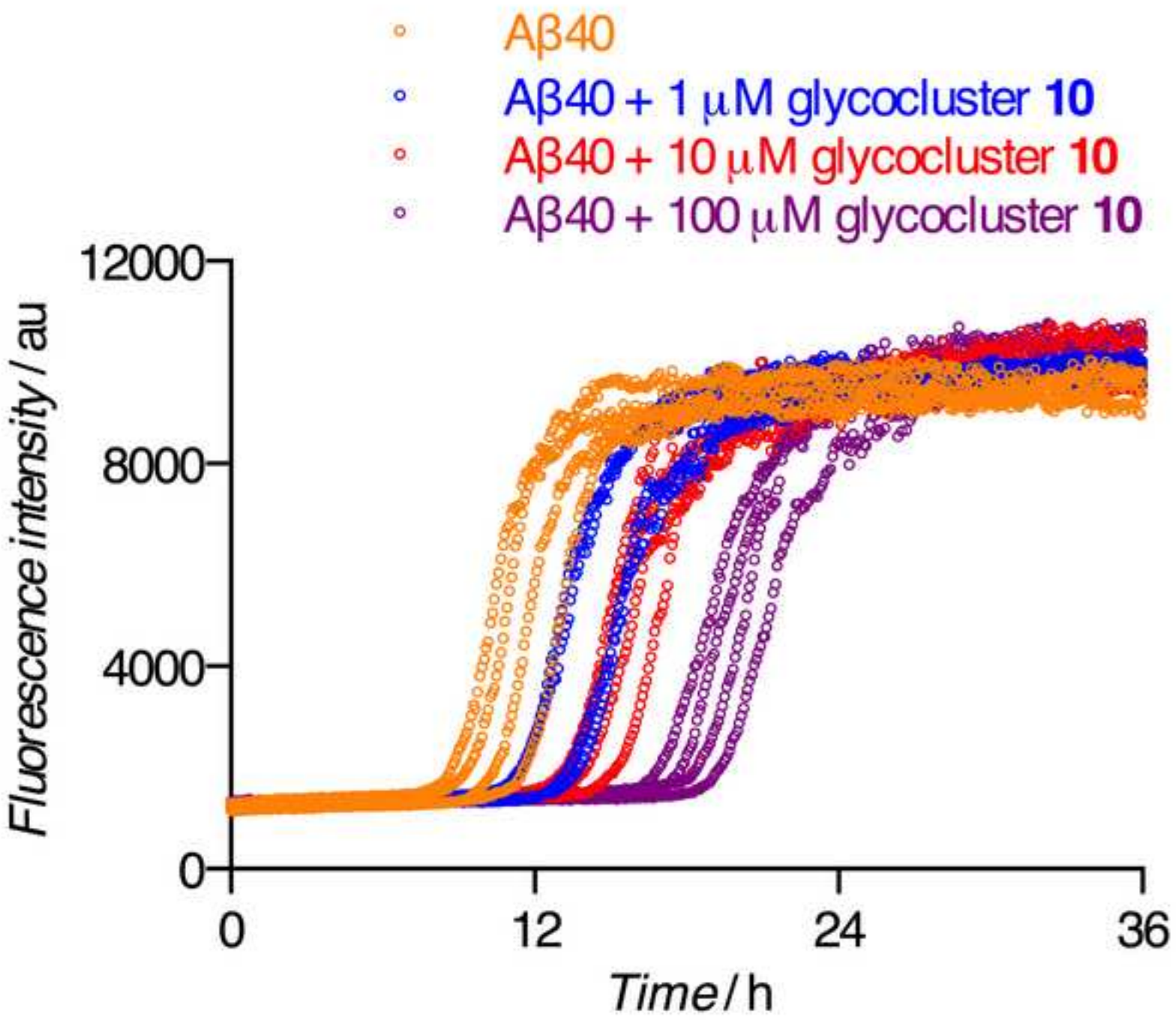

Fig 2

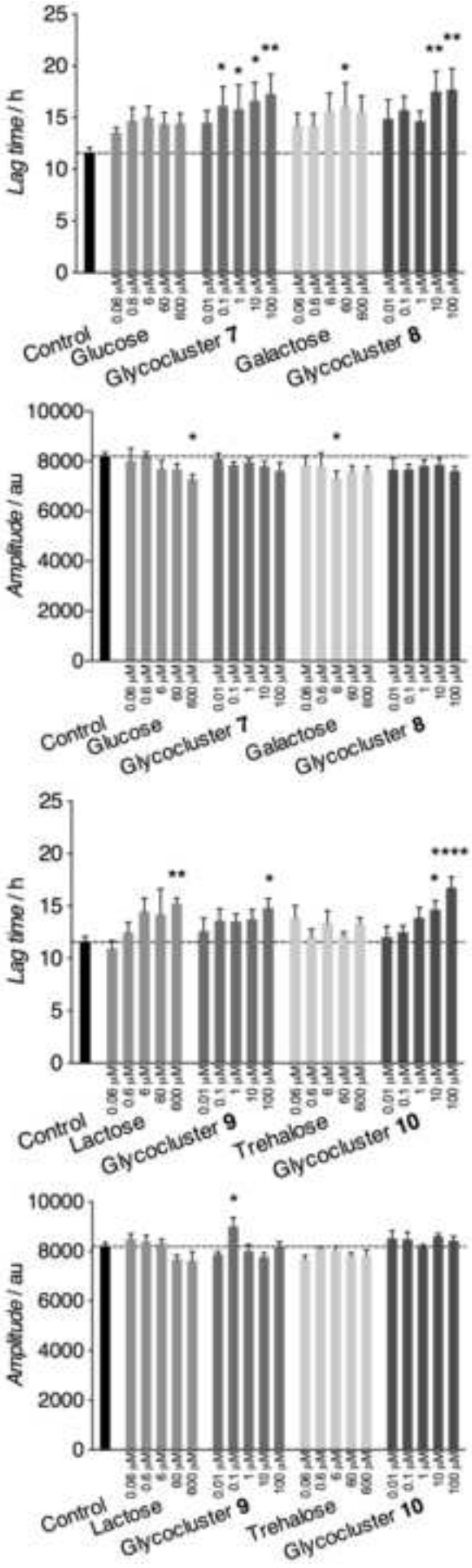

Fig 3

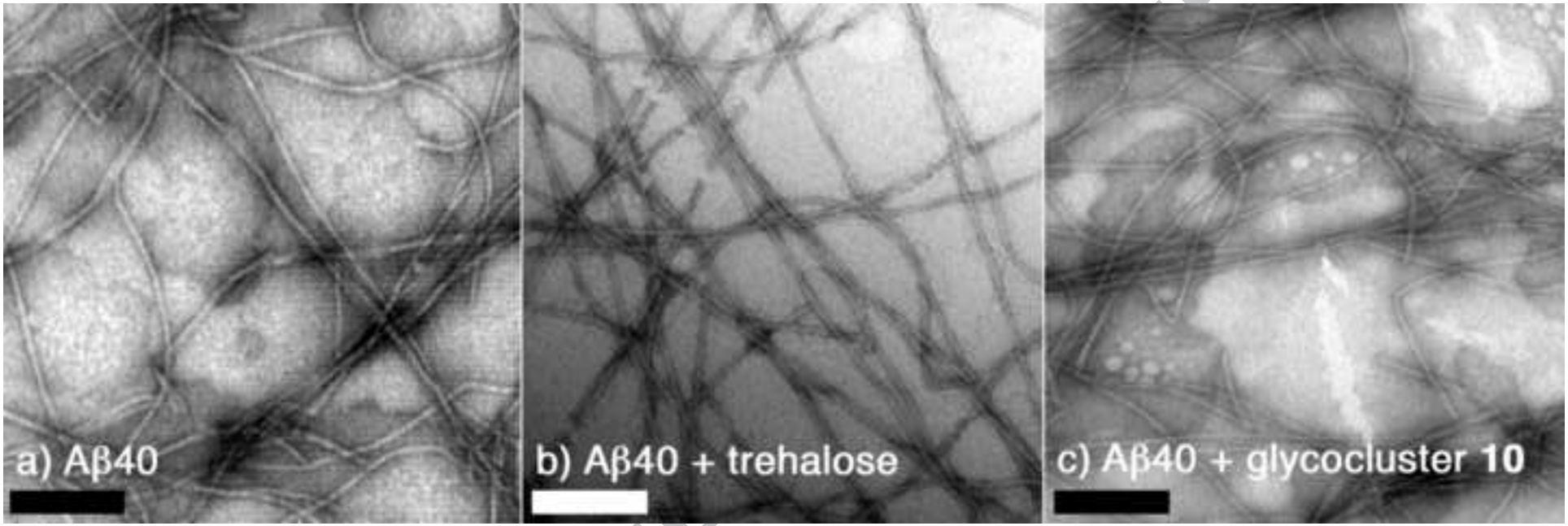

Fig 4